16th IMEKO TC4 Symposium
Exploring New Frontiers of Instrumentation and Methods for Electrical and Electronic Measurements
Sept. 22–24, 2008, Florence, Italy

Mass Contour Extraction in Mammographic Images for Breast Cancer Identification

Giulia Rabottino[1], Arianna Mencattini[1], Marcello Salmeri[1],
Federica Caselli[2], Roberto Lojacono[1]

[1] Department of Electronic Engineering, University of Rome "Tor Vergata",
[2] Department of Civil Engineering, University of Rome "Tor Vergata",
Viale del Politecnico, 1 – 00133 – Roma, Italy,
Phone: +39–06 72597368, Email: {rabottino, mencattini, salmeri, caselli, lojacono}@ing.uniroma2.it

Abstract **–** Mammography is the most effective tool now available for an early diagnosis of breast cancer. However, the detection of cancer signs in mammograms is a difficult task owing to the great number of non pathological structures which are also present in the image. It has been shown that in current breast cancer screenings 10%–25% of the tumors are missed by the radiologists. For this reason, a lot of research is currently being done to develop systems for Computer Aided Detection (CADe). Probably, some causes of the false–negative screening examinations are that tumoral masses have varying dimension and irregular shape, their borders are often ill–defined and their contrast is very low, thus making difficult the discrimination from parenchymal structures. Therefore, in a CADe system a preliminary segmentation procedure has to be implemented in order to separate the mass from background tissue. In this way, various characteristics of the segmented mass can be evaluated, which may be used in a classification step to discriminate pathological and negative cases. In this paper we describe an effective algorithm for massive lesions segmentation based on region–growing technique and we provide full details of the performance evaluation procedure used in this specific context.

I. Introduction

Among women worldwide, breast cancer is the most common cause of cancer death [1]. Mammography is still the best choice for screening of early breast cancer, since it is relatively fast, reasonably accurate, and widely available in developed countries. Because of the low contrast of mammographic images and the variable nature of the lesions, their interpretation is a difficult proceeding. For this reason, an automatic system can be a useful aid to the radiologist [2].

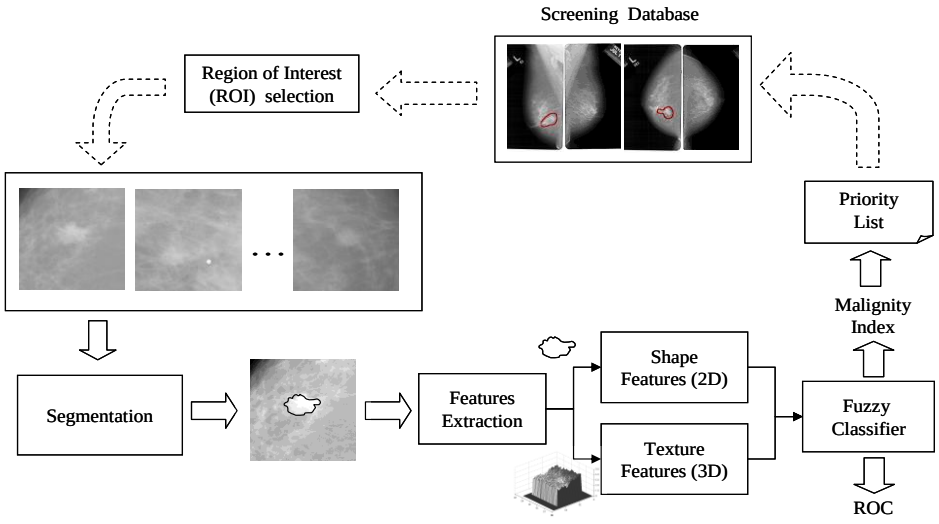

Figure 1. The whole system architecture.

We have implemented a whole detection and classification system. In this work we present, in particular, a fast and optimized region growing algorithm for the segmentation step aimed at finding the contour of the mass. This procedure is fundamental for the classification of massive lesions and can strongly influence its performance.
The whole system architecture is presented in Fig. 1. First, a Region of Interest (ROI) is selected from the mammographic image. The extraction is presently manually performed by the radiologist. Then a segmentation step is accomplished: first a suitable algorithm for enhancement is applied to the ROI to emphasize low contrast objects such as massive lesions, then the system automatically segment cancer signs, finding the lesion contour. The latter step is performed using a region growing algorithm. Finally, a classifier, based on fuzzy logic, using suitable features of shape and texture extracted from the segmented objects, works in order to assign a malignancy index to the lesions.
Obviously, the performance of the classification step is strongly influenced by the results of the segmentation. Consequently, a specific and effective mass contour extraction algorithm is needed in order to really aid radiologists in the detection and diagnosis of cancer. Nevertheless, the algorithm should be fast since the Computer Aided Detection system (CADe) should be able to identify tumoral lesions as a second human reader [3].

III. Contour extraction

In this section, we describe the main steps of the contour extraction of massive lesions by the region–growing algorithm. Then, the following section will address the problem of performance evaluation.
Many algorithms can be used for boundary extraction: *pixel–based* algorithms [4,5], processing only the intensity and loosing spatial information; *edge–based* algorithms [6], applying first or second order derivative to extract edges and reconstruct the boundary, not effective in the segmentation of low contrast objects; *region–based* algorithms [7,8], using both intensity, spatial and connectivity information to link pixels belonging to the boundary. Region–growing approaches exploit the important fact that pixels which are close together have similar gray values.
As already noted, a Region of Interest (ROI) is preliminary manually extracted by the radiologist.
The boundary extraction algorithm can be then summarized as follows: (1) *artifacts removal*, (2) *contrast enhancement*, (3) *region growing algorithm*, (4) *optimization.*
(1) *Artifacts removal.* Some images present bright and regular structures (artifacts) that can affect the region growing process. In fact, a bright luminance can influence region growing parameters altering the global segmented area. For this reason, it is useful to remove this kind of structures.
We base this step on the analysis of the ROI histogram. In case of presence of artifacts, the histogram presents an isolated peak in the high luminance zone and artifact removal is achieved by bringing back this peak in the range of intensities of the ROI. An example is shown in Fig. 2.

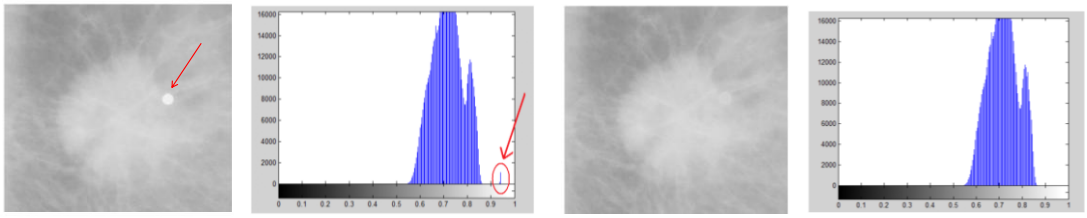

Figure 2. Artifacts removal.

(2) *Contrast enhancement*. The enhanced image is obtained by applying the non linear operator:

$$I_{en}(i,j) = \left(\frac{I(i,j)}{\max(I(i,j))} \right)^4$$

where $I(i,j)$ and $I_{en}(i,j)$ denote the pixel luminance of the original and enhanced images, respectively, and $\max(I(i,j))$ is the maximum intensity in the ROI. In this way, we penalize dark pixels (background) more than light pixels (mass). This operation does not saturate the processed image preserving all the useful information, but it is effective only after the artifacts removal. Results of this step will be shown in section III.

(3) *Region growing algorithm.* The algorithm starts from one pixel, called seed, and then, expands the

area around the seed to include nearby pixels falling within a threshold range. The main steps can be summarized as follows.

a. Choose the seed pixel. The seed is manually chosen approximatively at the center of the mass and its value is set to the average of the 15x15 neighboring pixels. In this way, the local intensity of the seed pixel does not influence the growing process.
b. Check the neighboring pixels and add them to the region if they are similar to the seed. The similarity condition we consider uses two thresholds Th_1 and Th_2 given by

$$Th_1 = I - (0.3 - K)\cdot \bar{I} \qquad Th_2 = I + (0.3 + K)\cdot \bar{I}$$

where $\bar{I}$ is the average value of luminance in the segmented region which changes at each growing step, and K is a parameter depending on both luminance and distance from the seed.
c. Repeat step 2 for each of the last added pixels; stop if no more pixels can be added.

(4) *Optimization.* The region growing algorithm is not applicable to high spatial resolution images because it would require too much computational time. For this reason, a variation of the algorithm is here proposed which enables to fulfill timing constraints. In particular, an image decimation makes possible a fast implementation of the region growing algorithm. We recall that in mammograms masses have considerable size (in the range [70–400] pixels with a spatial resolution of [43–50] μm). We uniformly divide the ROI in nonoverlapping regions of 3x3 pixels evaluating the average value of each square of the ROI. This value is assigned to the corresponding pixel in the decimated image. At this point, we apply the region growing algorithm on this decimated image obtaining an approximate contour. We then remap the contour in the original image, connect the pixels and iterate the algorithm only on these pixels to refine the contour. Obviously, this step would be unapplicable in images containing microcalcifications (diameter in the range [0.1–1] mm).

IV. Performance evaluation

As a validation, the proposed algorithm has been tested on mammographic images (LJPEG, gray–scale, 12/16 bit resolution) taken from Digital Database for Screening Mammography (DDSM) [9,10]. First results concerning the segmentation step and the extraction of mass boundary are provided. Figure 2 shows some examples of the mass contours.

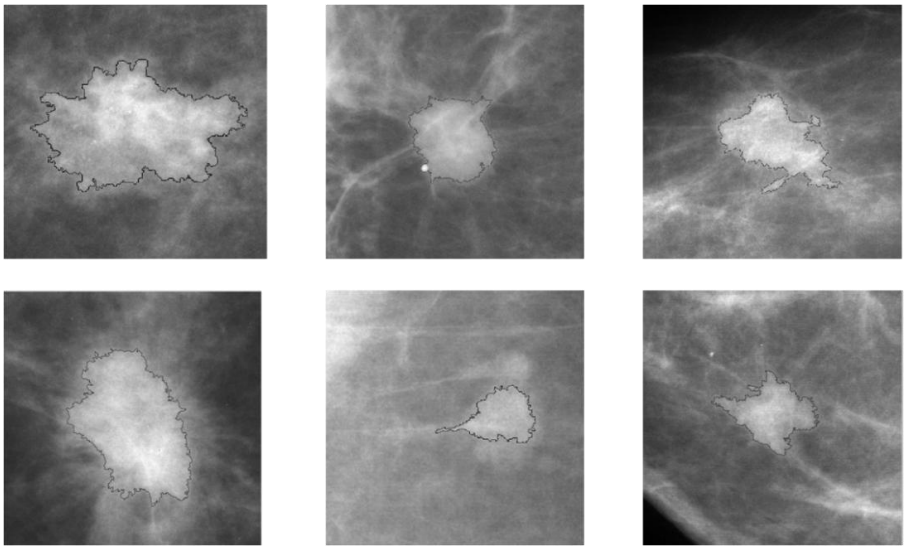

Figure 3. Contours extracted by region–growing.

There is no general consensus as to evaluate performance of an algorithm for medical image processing. However, various aspects should be considered [11]: (a) testing protocol, (b) testing regime, (c) performance indicators, (d) performance indices and metrics, (e) and image database.

(a) *Testing protocol.* Define the approach used for the algorithm testing: *visual assessment*, thus obtaining a qualitative impression of the results; *ground–truth* (if achievable), thus comparing the

results with those obtained by radiologist; *statistical evaluation,* using quantitative performances metrics and indexes.
(b) *Testing regime*. Define the strategy used for testing the images: in *exhaustive* methods every possible image in a database is considered; in *boundary value testing* only the most representative images are used for testing, in *random testing* images are chosen randomly in a database, and finally in *worst–case testing* only the anomalous (rare or unusual) images are used for testing.
(c) *Performance indicators*. There exist seven parameters that characterize an algorithm: robustness, sensitivity, adaptability, accuracy, precision, reliability, efficiency.
(d) *Performance indexes and metrics.* Quantitative measures that allows us to evaluate the performance of a specific algorithm in a particular context. For segmentation algorithms *performance indexes* are:

- TP (true positive) the set of pixels correctly classified as features in the segmented image,
- TN (true negative) the set of pixels correctly classified as background in the segmented image,
- FP (false positive) the set of pixels classified as features in the segmented image and as background in the ground–truth,
- FN (false negative) the set of pixels classified as background pixel in the segmented image and as features in the ground–truth.

Performance metrics are parameters strongly related to the algorithm and to the considered images. For example, medical image enhancement uses CII (contrast improvement index) [12], NAI (noise amplification index) [12], PSNR (peak to signal ratio) [13,14], ASNR (Average signal to noise ratio) [13,14], while, for mass segmentation, Hausdorff distance, CM and CR (area completeness and correctness [15] are considered.
(e) *Image database*. Performance evaluation is biased by *image database* used for testing. Two databases of mammographic images are presently publically available: DDSM (Digital Database for Screening Mammography) containing more than 3000 images, 12–16 bpp, with a spatial resolution of 43–50 μm and a wide variety of pathological and normal cases; and MiniMIAS database [16] with a spatial resolution of 80–100 μm that is not very representative for every pathological case. It is well known that comparing two algorithm testing them on two different databases is not correct. Moreover, an extreme variability can be encountered also within the same database, according to different breast tissues: fatty, extremely dense, scattered fibroglandular densities, etc.
Following the above description of the testing protocol and procedure, we now consider the issues of mass segmentation and boundary extraction described in the first part of the paper.
Going through the whole segmentation algorithm we can evaluate each step as follows.
The *first step* is the *artifact removal*. Obviously artifact removal performance has to be evaluated by visual assessment, since the ground–truth is not achievable.
The *second step* is the image contrast enhancement, performing a nonlinear histogram stretching by elevating the normalized intensity to the power of four. Performance metrics here used are CII, PSNR, and ASNR. They are reported in Tab. 1 for the image represented in Fig. 4, also showing the extraction of foreground and background needed for the indexes evaluation.

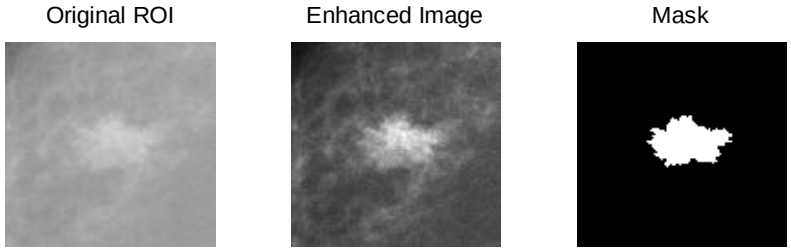

Figure 4. Image enhancement effect and segmentation mask.

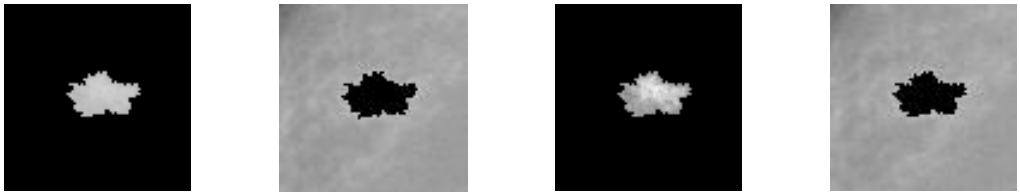

Figure 5. Foreground and background before (left and centre–left) and after (centre–right and right)

contrast enhancement by nonlinear histogram stretching.

C_{Orig}	C_{Proc}	CII	$PSNR_{Orig}$	$PSNR_{Proc}$	$ASNR_{Orig}$	$ASNR_{Proc}$
0.0933	0.3537	3.7891	5.8174	9.7123	3.7282	5.3279

Table 1. Contrast improvement and image quality indexes.

The *third step* deals with contour extraction by region growing algorithm. In this case we both evaluate some performance indexes for the algorithm itself and the final result of boundary extraction. The algorithm has been evaluated in term of *efficiency, adaptability, and robustness.* In particular:

- *Efficiency* in term of computational time and space is increased of an order of magnitude thanks to the preliminary decimation. Globally, if the initial number of pixels to be examined is of order of N^2, about 2 (N/3) (N/3) ~ N^2/9 pixel are left after the decimation (N is in the range [70 – 300]).
- *Adaptability* is evaluated by applying the algorithm on 200 images taken from DDSM containing malignant or benign massive lesion, with different shape, size, contrast, border spiculation. The algorithm works properly in virtually all cases.
- *Robustness* is evaluated by applying the algorithm with and without a preliminary denoising step. The two visual results are found to be comparable.

The quality of boundary extraction is assessed by taking as a Ground–Truth a manual extraction of the contour. An example is presented in Fig. 6. We consider as TP the segmented area, FP the area not identified and FN the area that has been erroneously identified. These regions are shown in Fig. 7 for the same mass considered in Fig. 6. Boundary extraction results are then evaluated by computing CM (Completeness) and CR (Correctness), defined as:

$$CM = \frac{TP}{TP + FN} \qquad CR = \frac{TP}{TP + FP}$$

In particular, completeness is the percentage of the Ground–Truth region which is detected by the segmented region, while the correctness is the percentage of correctly extracted breast region. For the example in Fig. 6 and 7 we obtain CM = 0.8834 and CR = 0.9338.

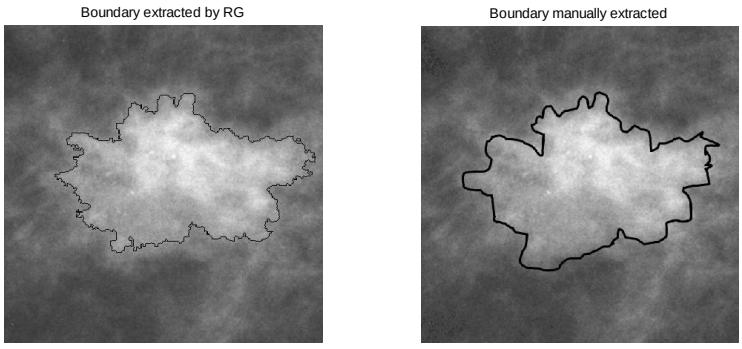

Figure 6. Contour extracted by Region–growing algorithm (left) and manually extracted (right).

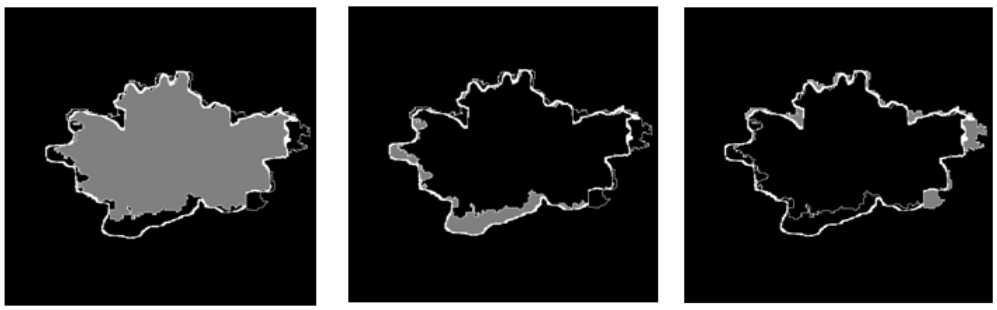

Figure 7. TP (top–left), FN (centre), FP (right) identified by gray regions.

The DDSM images come from Screen Film Mammography and are digitalized by three kinds of Scanner Devices that are fully metrological characterized in term of standard deviation and optical

density function on the web site [9,10]. The database contains many images that are very representative for many pathological situations both for masses and microcalcifications. Images have the highest spatial resolution and bit depth among other public database available thus allowing us a full and detailed performance evaluation of the proposed segmentation algorithm.
We finally conclude that the performance of a forthcoming classification step will be further evaluated by specific metrics and indicators. In particular in that context, ground–truth will be represented by the diagnosis of the massive lesions made by radiologists. Then, the concept of TP, TN, FN, and FP will be readapted to the scope of classification.

IV. Conclusions

The contour extraction of tumoral masses is a critical step in any computer aided detection system. In fact, the next steps of features extraction and classification depend, in a fundamental way, on the performance of the boundary extraction. In particular, the spiculation, boundary roughness and irregularity of the extracted contour are typical features of malignant masses. The proposed algorithm performs a contour searching that is not dependent on the mass size and maintains all the information on the irregularity of the boundary. Moreover, by an optimized implementation, the new method also allows a fast application that is not possible with the classical region growing algorithms. In order to validate the whole mass segmentation algorithm, we also investigate the commonly used performance indicators and metrics, using them in order to test the algorithm on mammographic images taken from the public digital database DDSM.

References

[1] World Health Organization (Feb 2006). Fact sheet No. 297: Cancer. Retrieved on 2007–04–26.
[2] A. Mencattini, M. Salmeri, R. Lojacono, M. Frigerio, F. Caselli, “Mammographic images enhancement and denoising for detection of tumoral signs using dyadic wavelet processing”, *IEEE Trans. on Instrumentation and Measurement*, vol. 57, n. 7, pp. 1422–1430, Jul 2008.
[3] J. Dinnes, S. Moss, J. Melia, R. Blanks, F. Song, J. Kleijnen, “Effectiveness and cost–effectiveness of double reading of mammograms in breast cancer screening: Findings of a systematic review”, *The Breast*, vol. 10, pp. 455–463, 2001.
[4] H. D. Li, M. Kallergi, M. Clarke, L.P. Jain, V.K. Clark, “Markov random field for tumor detection in digital mammography”, *IEEE Trans. on Medical Imaging*, vol. 14, n. 3, pp. 565–576, Sep 1995.
[5] T. Matsubara, H. Fujita, T. Endo, K. Horita, C. Kido, M. Ikeda, T. Ishigaki, “Development of mass detection algorithm based on adaptive thresholding technique in digital mammograms”, *Inter. Workshop on Digital Mammography*, pp. 391–396, 1996.
[6] W. E. Polakowski, D. A. Cournoyer, S. K. Rogers, M. P. Desimio, D. W. Ruck, J. W. Hoffmeister, R. A. Raines, “Computer–aided breast cancer detection and diagnosis of masses using difference of gaussians and derivative–based feature saliency”, *IEEE Trans. on Medical Imaging*, vol. 16, n. 6, 1997.
[7] R. Zwiggelaara, T. C. Parra, W. Hutt, C. J. Taylo, S. M. Astley, C. R. M. Boggis, “Model–based detection of spiculated lesions in mammograms”, *Medical Image Analysis*, vol. 3, n. 1, pp. 39–62, 1999.
[8] I. N. Bankman, T. Nizialek, I. Simon, O. B. Gatewood, I. N. Weinberg, W. R. Brody, “Recent advances in breast imaging, mammography, and computer–aided diagnosis of breast cancer”, chapter *Algorithms for segmenting small low–contrast objects in images*, pp. 723–738, SPIE Press, Bellingham, USA, 2006.
[9] M. Heath, K.W. Bowyer, D. Kopans, R. Moore, P. Kegelmeyer, “Digital Mammography”, chapter *Current status of the Digital Database for Screening Mammography*, pp. 457–460, Kluwer Academic Publishers, 1998.
[10] University of South Florida. University of South Florida digital mammography home page, 2000.
[11] M. A. Wirth, “Performance Evaluation of CADe Algorithms in mammography”, chapter *Recent advances in breast imaging, mammography, and computer aided diagnosis of breast cancer*, pp. 639–699, SPIE Press, Washington, USA, 2006.
[12] P. Sakellaropoulos, L. Costaridou, G. Panayiotakis, “A wavelet–based spatially adaptive method for mammographic contrast enhancement”, *Phys. Med. Biol.*, vol. 48, pp. 787–803, 2003.
[13] H. Li, K. Liu, S. Lo, “Fractal modeling of mammogram and enhancement of microcalcifications”, *Nuclear Science Symposium & Medical Imaging Conference*, vol. 3, Nov 1996.
[14] H. Li, K. Liu, S. Lo, Fractal modeling and segmentation for the enhancement of microcalcifications in digital mammograms, *IEEE Trans. on Medical Imaging*, vol. 16, n. 6, pp. 785–798, 1997.
[15] M. Wirth, D. Nikitenko, J. Lyon, “Segmentation of the breast region in mammograms using snakes”, *ICGST Int. J. Graphics Vision Image Process.*, vol. 2, pp. 45–54, 2005.
[16] J. Suckling, et al., J. Parker, D.R. Dance, S. Astley, I. Hutt, C.R.M. Boggis, I. Ricketts, E. Stamatakis, N. Cerneaz, S.–L. Kok, P. Taylor, D. Betal, J. Savage, “The mammographic image analysis society digital mammogram database”, *Intern. Workshop on Digital Mammography*, vol. 1069, pp. 375–378, 1994.